What are the differences in yield formation among two cucumber (Cucumis sativus L.) cultivars and their F1 hybrid?

Xiu-Juan Wang, Meng-Zhen Kang, Xing-Rong Fan, Li-Li Yang, Bao-Gui Zhang, San-Wen Huang, Philippe de Reffye, Fei-Yue Wang

RESEARCH ARTICLE

What are the differences in yield formation among two cucumber (*Cucumis sativus* L.) cultivars and their F$_1$ hybrid?

WANG Xiu-juan[1, 2], KANG Meng-zhen[1, 3], FAN Xing-rong[4], YANG Li-li[5], ZHANG Bao-gui[6], HUANG San-wen[7], Philippe DE REFFYE[8], WANG Fei-yue[1, 9]

[1] *The State Key Laboratory of Management and Control for Complex Systems, Institute of Automation, Chinese Academy of Sciences, Beijing 100190, P.R.China*

[2] *Beijing Engineering Research Center of Intelligent Systems and Technology, Institute of Automation, Chinese Academy of Sciences, Beijing 100190, P.R.China*

[3] *Innovation Center for Parallel Agriculture, Qingdao Academy of Intelligent Industries, Qingdao 266109, P.R.China*

[4] *School of Computer Science and Information Engineering, Chongqing Technology and Business University, Chongqing 400067, P.R.China*

[5] *College of Information and Electrical Engineering, China Agricultural University, Beijing 100083, P.R.China*

[6] *College of Land Science and Technology, China Agricultural University, Beijing 100193, P.R.China*

[7] *Agricultural Genomes Institute at Shenzhen, Chinese Academy of Agricultural Sciences, Shenzhen 518124, P.R.China*

[8] *AMAP, University Montpellier, CIRAD, CNRS, INRA, IRD, Montpellier 34000, France*

[9] *The School of Computer and Control Engineering, University of Chinese Academy of Sciences, Beijing 100049, P.R.China*

Abstract

To elucidate the mechanisms underlying the differences in yield formation among two parents (P$_1$ and P$_2$) and their F$_1$ hybrid of cucumber, biomass production and whole source–sink dynamics were analyzed using a functional–structural plant model (FSPM) that simulates both the number and size of individual organs. Observations of plant development and organ biomass were recorded throughout the growth periods of the plants. The GreenLab Model was used to analyze the differences in fruit setting, organ expansion, biomass production and biomass allocation. The source–sink parameters were estimated from the experimental measurements. Moreover, a particle swarm optimization algorithm (PSO) was applied to analyze whether the fruit setting is related to the source–sink ratio. The results showed that the internal source–sink ratio increased in the vegetative stage and reached a peak until the first fruit setting. The high yield of hybrid F$_1$ is the compound result of both fruit setting and the internal source–sink ratio. The optimization results also revealed that the incremental changes in fruit weight result from the increases in sink strength and proportion of plant biomass allocation for fruits. The model-aided analysis revealed that heterosis is a result of a delicate compromise between fruit setting and fruit sink strength. The organ-

level model may provide a computational approach to define the target of breeding by combination with a genetic model.

1. Introduction

Cucumber (*Cucumis sativus* L.) is a very popular vegetable plant worldwide, and its yield components comprise the number, weight and quality of individual fruits (Marcelis 1992). Hybrid vegetable technology is one of the best options to improve cucumber yield. Hybrid vigor can be expressed by the total yield and increased yield due to the large number of fruits/plants (Ghaderi and Lower 1978). Yield and fruit quality are some of the most frequent traits influenced by heterosis. Heterosis or hybrid vigor is commonly known as the superior performance of hybrid organisms compared with either of their parents (Birchler 2015). In cucumber, Hayes and Jones (1916) first observed heterosis in fruit size and fruit number per plant. Ghaderi and Lower (1978) suggested that heterosis in yield components such as the number or weight of leaves, branches, and roots should have a direct effect on fruit yield. F_1 hybrids may have greater photosynthetic activity than their parents, thus leading to a higher yield.

Crop yield is the result of the interactions of genetic and environmental factors. Breeders have proposed the concept of an ideal plant (ideotype) adapted to a target environment. For cucumber, a heliophile crop, dry matter production through photosynthesis is one of the most important processes to consider when characterizing an ideotype. Internode length, leaf size and leaf angle are three important traits of the ideal cucumber plant architecture (Falster and Westoby 2003; Sarlikioti *et al*. 2011). Breeding for yield mainly utilizes hybrid vigor to change some plant morphological traits by hybrid breeding, thus improving the yield, cultivar and resistance (Xie *et al*. 2009). A major difficulty lies in decomposing the complex interactions between genotype and environment because the main phenotypic traits (e.g., yield, plant height, organ number and size) integrate multiple internal morphological and physiological processes and external interactions with field and climatic conditions (Letort *et al*. 2008).

Heuvelink *et al*. (2007) reported that using plant models allows the evaluation of newly available genotypes by analyzing their performance and identifying the most influential parameters to improve yield under various environmental conditions. Many plant growth models have been developed to increase our knowledge of plants, improving agricultural practices and environmental

optimization and control (Wu *et al*. 2012; Fan *et al*. 2015). Studies of the potential of linking growth models to quantitative genetics aim to integrate genetic knowledge in plant growth models considering the effect of the environment (Hammer *et al*. 2005; Letort *et al*. 2008; Xu *et al*. 2011; Yin *et al*. 2016; Chew *et al*. 2017). If the model parameters themselves can be viewed as different quantitative traits, they should have high heritability because they are expected to be less dependent on the environmental conditions and to show more direct gene expression (Letort *et al*. 2008). Thus, it is easier to analyze the genetic effects using model parameters than using traditional traits. Moreover, optimization processes allow the determination of key parameters influencing yield, even when complex genetic correlations are introduced. However, plant growth model selection will be a crucial step.

Functional–structural plant models (FSPMs) explicitly describe the development of a plant structure over time as governed by physiological processes that, in turn, depend on environmental factors (Vos *et al*. 2007). Such models dynamically simulate plant systems, allowing for feedback between processes at the level of individual organs and functioning of the plant as a whole (Vos *et al*. 2010). The features of FSPMs are interesting for studying fruit setting in horticultural plants (Wubs *et al*. 2009). Based on botanical knowledge and source–sink regulation rules, the FSPM GreenLab is a generic model that can simulate interactions among the fruit set (e.g., position, number and size), biomass production and allocation to better understand the dynamics of biomass production and morphogenesis among cucumber cultivars. Furthermore, one interesting feature of the GreenLab Model is that the Model parameters can be adjusted globally by fitting model outputs to corresponding measured organ biomass (Christophe *et al*. 2008) thanks to its mathematical formalism; this is a demanding and critical step in developing and applying a model (Seidel *et al*. 2018). The GreenLab Model has been applied to various plants, including maize (Ma *et al*. 2008), tomato (Kang *et al*. 2011), sweet pepper (Ma *et al*. 2011), and chrysanthemum (Kang *et al*. 2012). However, none of these plants has been used to analyze heterosis between parents and F_1 hybrids.

The aim of the study was to analyze the processes underlying the different biomass production levels between two parents (P_1 and P_2) and their F_1 hybrid of cucumber using a modeling approach. First, the GreenLab Model was calibrated with the data of the two parents and their

F_1 hybrid to more deeply understand the differences among their development and growth processes with the estimated model parameters; second, a particle swarm optimization algorithm (PSO) was applied to investigate the relationship between the fruit setting and source–sink ratio by simultaneously optimizing the source–sink parameters and fruit positions and numbers. This model-based analysis thus provides a new tool to better understand the heterosis phenomenon.

2. Materials and methods

2.1. Experiment setup and measurements

Plant materials Cucumber (*Cucumis sativus* L.) seeds were provided by the Institute of Vegetables and Flowers, Chinese Academy of Agricultural Sciences. The large-leaf line (*C. sativus* var. *sativus*) DF-32 (P_1), the small-leaf line (*C. sativus* var. *hardwickii*) XF-24 (P_2) and their hybrid (F_1) were cultivated in a greenhouse of China Agricultural University (40.01°N, 116.28°E) from March to July 2010.

The parent P_1 is a late-maturing cultivar; the first female flower is located at the 15th–16th phytomer (counting from the base). This cultivar produces large blades and large fruit with a low fruit-set rate. The parent P_2 is an early-maturing cultivar; the first female flower is located at the 3rd–5th phytomer. This cultivar produces small blades and small fruit with a high fruit-set rate. The traits of the F_1 hybrid are intermediary (Fig. 1).

The two parents and F_1 hybrid were sown on March 9, 2010. Cucumber seedlings with four leaves were implanted into 25-cm pots on April 10, 2010. The pots were filled with 70% peat, 20% vermiculite and 10% pearlite. Next, 20,

20 and 10 pots of plants were planted for P_1, P_2 and F_1, respectively. There was no water or nutrient stress. All tendrils and side shoots were pruned to allow monopodial growth. Measurements were performed on two plants in the middle rows with at least one border plant on each side. The fruits were harvested every three or four days.

Measurements The environmental conditions, namely, temperature, humidity and light intensity, were monitored during plant growth in the greenhouse to analyze their effects. Both destructive measurements and continuous nondestructive observations were carried out. Continuous observations were performed on six plants for two parents and F_1 hybrid, twice per week, with detailed topological observations on the number of leaves, phytomer ranks of flowers on the main stem, and stage of development (flower bud, flower and fruit or abortion) at each flower position, in order to describe dynamic fruit setting for two parents and F_1 hybrid.

In destructive measurements, two cucumber plants for two parents and F_1 hybrid were selected to measure the dry weight of individual organs (internode, blade, petiole and root) and blade surface for each sampling. In total, six samplings were made during the growing period (S1, 10 April; S2, 26 April; S3, 17 May; S4, 31 May; S5, 16 June; and S6, 3 July). The measured data were used to estimate the source–sink parameters of the model for two parents and F_1 hybrid.

2.2. GreenLab Model

GreenLab is a generic plant model that simulates two basic plant processes: development (organogenesis) and growth (organ expansion) (Yan *et al.* 2004). At each time
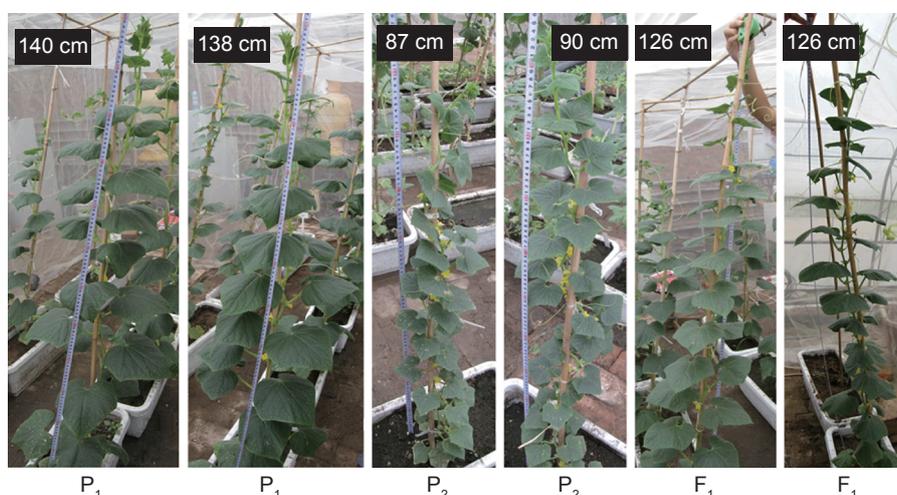

Fig. 1 Pictures of the parents P_1 and P_2 and their F_1 hybrid of cucumbers on May 31, 2010.

interval, called the growth cycle (GC, the period between the sequential emergence of leaves on the main stem of a plant), the plant structure is updated according to the organogenesis model. Organogenesis is simulated with a dual-scale automaton (Yan et al. 2002), which gives the number of organs at each cycle that participate in biomass production and allocation.

Modeling biomass production In the GreenLab Model, at the ith GC, the biomass production of a plant $Q(i)$ is calculated using eq. (1) (Guo et al. 2006):

$$Q(i)=PET(i)\cdot\mu\cdot S_P\left(1-\exp\left(-k\frac{S(i)}{S_P}\right)\right) \tag{1}$$

where i is the age of the plant in GC. $PET(i)$ (mm per GC) is the potential evapotranspiration during the ith GC that is affected by several microclimate conditions (light, temperature and vapor pressure deficit) (Allen et al. 1998). The PET of a GC is summed from daily PET values, the duration depending on the daily temperature and phyllochron per cycle; S_P (cm^2) is the ground maximal projection area of the plant, linked to the density of planting (Ma et al. 2008); μ (g cm^{-2} mm^{-1}) estimates the water use efficiency, expressing produced biomass by plant evapotranspiration per unit of water (Kang et al. 2011); k is the light extinction coefficient, set to an empirical value of 1; $S(i)$ is the total functioning leaf area at the ith GC, summed from the individual leaf area in the model. Each leaf area is computed from its biomass and a specific leaf weight, the latter being assessed directly from the data. Because the biomass of each leaf is dependent on the global plant demand during its expansion, it can be affected by concurrent events such as the fruit set. The initial biomass $Q(0)$ is from the seed.

Modeling biomass partitioning The model is based on the hypothesis that dry matter partitioning is regulated by the sink strengths of the plant organs. The sink strength of an organ is defined here as the potential growth capacity, i.e., the biomass at nonlimiting assimilate supply (Marcelis 1994). Biomass is distributed among growing organs according to their own sink strength. The sink strength of organ o of age j is calculated by eq. (2):

$$p_o(j)=P_o\,f_o(j) \tag{2}$$

where P_o is the organ sink strength, and o represents the organ type (b, blade; p, petiole; in, internode; f, female). In this study, we set the maximum measured value of fruit, that is, P_f equals 14.6, 7.6 and 12.3 g for the parents P_1 and P_2 and hybrid F_1, respectively, as the reference potential sink strength. The sink strengths of other organs (P_b, P_p and P_{in}) are hidden parameters to be estimated from the plant data. Thus, the sink strength has units (g per GC) and represents the organ's ability to compete for assimilates in each GC. Because each organ has different needs for biomass during its lifetime, function $f_o(j)$ is defined as the

organ sink variation, described empirically by a discrete *Beta* function as in eq. (3):

$$f_o(j)=\begin{cases} g_o^j/\mu_o & 1\leq j\leq t_o \\ \\ 0 & j>t_o \end{cases} \tag{3}$$

where

$$g_o^j=\left(\frac{j-0.5}{t_o}\right)^{a_o-1}\left(1-\frac{j-0.5}{t_o}\right)^{b_o-1}$$

$$\mu_o=\sum_{j=1}^{t_o} g_o^j \qquad o\text{=b, p, in, f}$$

This function gives the shape of the organ sink variation curve at a constant biomass supply. The product $P_o f_o(j)$ gives the demand of organ o with age j in the plant. Given the expansion duration t_o and one of the control parameters a_o=2, another control parameter b_o was estimated from the plant data for each type of organ. This constraint is empirical and generally yield good results for different organs and plants (Guo et al. 2006; Kang et al. 2011). The larger the value of b_o is, the faster the expansion is. Appendix A shows different curve shapes of $f_o(j)$ depending on the values of parameters a_o and b_o, which could differ among organ types and plant species. The duration of growth t_o of organ o can be observed directly from measurements, which is approximated to be 20 cycles.

Summing the sink strength of all organs, we obtain the total demand of plant $D(i)$ at the ith GC:

$$D(i)=\sum_o P_o\left(\sum_{j=1}^i N_o(i,j)\,f_o(j)\right) \tag{4}$$

where $N_o(i,j)$ is the number of organs o of age j at plant age i. In the cucumber plant here, for leaves and internodes, this value is 1; for the fruit, it can be 0 or 1, depending on whether a fruit is set at the phytomer rank.

According to the sink strength, the biomass acquired by the organ of age j at the ith GC is:

$$\Delta q_o(i,j)=\frac{P_o f_o(j)}{D(i)}Q(i) \tag{5}$$

In eq. (5), the dynamic source–sink ratio $Q(i)/D(i)$, simply written as Q/D. It reflects the competition level in the plant, showing the biomass availability for each organ. According to eq. (5), larger Q/D values during the expansion of an organ produce a larger final biomass. This ratio can be computed by the model recurrently when all parameter values are known. The source–sink ratio at the fruit set is quantified by computing this ratio when each fruit appears, and a threshold is given as s_{low}. For cucumber, a fruit will possibly appear at each node, but only some positions can set a fruit; therefore, when the position sets a fruit, the plant demand (D) increases, then the ratio Q/D decreases and is lower than the threshold. Therefore, some later produced fruit may abort while the competition for assimilates

increases. Thus, spatial fruit position can be determined by the source–sink ratio (Ma *et al*. 2011).

Summing the biomass of all individual organs of the same property produces the total biomass of organs that can be obtained by experimental measurements. The biomass of an organ o is the accumulated biomass of the organ of age j at the ith GC:

$$q_o(i, j)=\sum_{k=1}^{j}\Delta q_o(i-j+k, k) \quad (i\geq j) \tag{6}$$

Accordingly, the total weight of the fruit at the final harvest, denoted by W_f (g/plant), is computed by eq. (7):

$$W_f=\sum_{j=1}^{t_f}N_f(N, j)\,q_f(N, j) \tag{7}$$

where t_f (unit: GC) is the fruit functioning duration, and N is the final GC (or maximal GC) of the plant.

2.3. Parameter estimation of GreenLab

In GreenLab, the parameters are classified into two categories: measurable parameters (e.g., functioning duration of blades, number of organs emerged at each GC) and hidden parameters that cannot be measured directly in the field (e.g., organ sink strength). The hidden parameters are estimated by minimizing the difference between the measured data and corresponding simulation results. A generalized nonlinear least-square method (GLSQR) adapted from the Levenberg-Marquardt algorithm is used for estimation (Zhan *et al*. 2003). Model computation and model fitting on experimental data were conducted using the open-source GreenScilab Software.

A common set of parameters (Table 1) is estimated simultaneously by fitting the plant data at different development stages, which is called multifitting. For directly measurable parameters, following the observations, the organ expansion duration (from appearance to stop growing) was set to 20 GCs, while the organ function duration (from appearance to death) was set to 40 GCs for the blade, petiole, internode and fruit according to the data of continuous observations. Leaf thickness was estimated as the ratio of the leaf fresh mass to surface area (Wright and Westoby 2002). It plays an important role in leaf and plant functioning and is related to species' strategies of resource acquisition and use (Vile *et al*. 2005).

2.4. Data analysis

Statistical analyses were performed using R2.11.1 (Copyright (C) 2010, the R Foundation for Statistical Computing). Analysis of variance (ANOVA) was used to assess the differences in phyllochron between the parents and F_1 hybrid.

2.5. Maximization of the fruit weight

To clarify the origin of heterosis, a PSO algorithm was applied to analyze whether the fruit setting could be related to the dynamic of the source–sink ratio. First, based on the estimated source–sink parameters, the fruit positions are optimized by setting different numbers of fruit per plant for the parents P_1 and P_2 and hybrid F_1 to analyze the effect of the sink organ on potential biomass production; second, both the source–sink parameters and positions of the fruit per plant were synchronously optimized using different numbers of fruits per plant to check the potential augmentation of yield.

The optimization objective was to maximize the total weight of the fruit for each plant. Assuming one fruit for one position, the mathematical formalism of the optimization problem is given by the following eq. (8):

Maximize W_f

$$\text{Subject to } 1\leq\sum_{i=1}^{N}\text{posFruit}(i)\leq NF \tag{8}$$

where posFruit(i) is a binary (0/1) variable depending on whether a fruit is set at the phytomer rank, which corresponds to the function of $N_o(i, j)$ in eq. (4) for the fruit; $\sum_{i=1}^{N}$posFruit(i) gives the total number of fruits per plant; NF is the maximum number of fruits; and W_f is a function of posFruit(i) and q_f (eq. (7)). A PSO algorithm is used to solve the optimization problem (Qi *et al*. 2010).

3. Results

3.1. Experimental results

Phyllochron The phyllochron shows no significant difference between the parents (P_1 and P_2) and the F_1 hybrid (ANOVA, $df=2$, $F=0.085$, $P>0.5$), as shown in Fig. 2.

Table 1 Source–sink parameters identified from the measurement data using the GLSQR method

Parameter[1]	Definition	Unit
P_b, P_p, P_{in}	Organ sink strength (eq. (2))	g
b_b, b_p, b_{in}, b_f	Organ sink variation parameter (eq. (3))	–
S_P	Characteristic surface of an individual plant (eq. (1))	cm^2
μ	Water use efficiency (eq. (1))	g cm^{-2} mm^{-1}
s_{low}	A threshold, fruits appear at GC t if source–sink ratio $Q_t/D_t>s_{low}$	–

[1] b, blade; p, petiole; in, internode; f, fruit.

This means that the development speed is similar, and we can use the same time step in the model to compute the source–sink parameters.

Because the environmental factors were considered by combining the daily PET values in eq. (1) of the model, the potential evapotranspiration (PET) per cycle was calculated by accumulating daily PET inside a GC according to the daily temperature, light intensity and air humidity (Fig. 3).

Vegetative organ biomass The biomass and sizes of organs from a given type (leaves, petioles and internodes) vary along the stem within one plant and are different at the same phytomer rank for two parents and F_1 hybrid. The plants of parent P_1 had the largest organ biomass for the internode, blade and petiole. In contrast, parent P_2 had the smallest organ sizes, while hybrid F_1 showed intermediate values, as shown in Fig. 4. Furthermore, the averaged plant heights and internode diameters showed similar patterns ($P_1>F_1>P_2$) (Table 2).
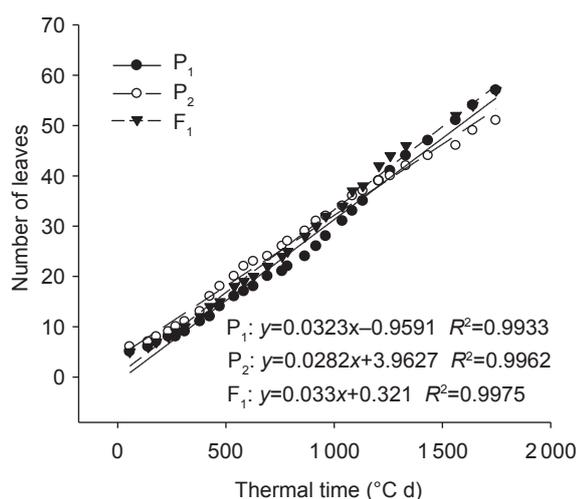

Fig. 2 Relationship between the leaf number and thermal time for the parents P_1 and P_2 and F_1 hybrid during plant development.
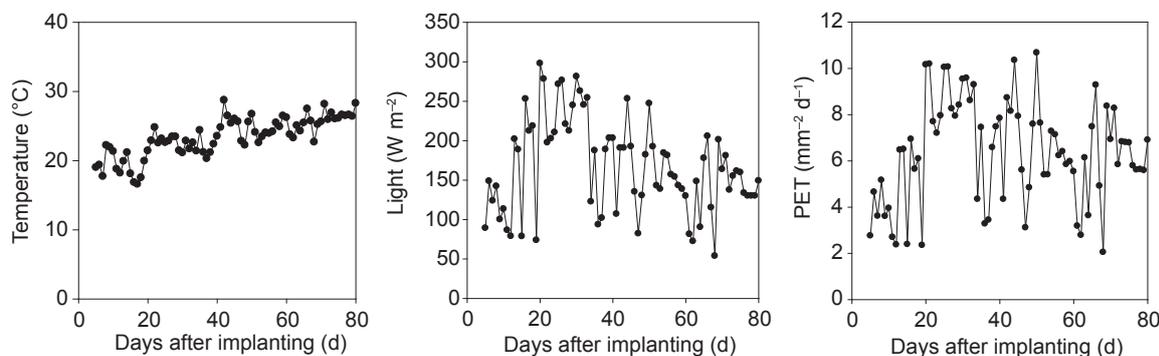
Fruit setting and fruit biomass According to the observation, the first fruit appeared at the phytomer ranks 15–16, 3–5 and 10–12 for parents P_1 and P_2 and hybrid F_1, respectively, i.e., the first fruit set was the earliest in P_2, latest in P_1 and that of F_1 was between them ($P_1>F_1>P_2$). The harvested mean final number of fruit per plant for parents P_1 and P_2 and hybrid F_1 showed an inverse trend ($P_1<F_1<P_2$). The mean dry weights of individual fruit were $P_1>F_1>P_2$ (Table 3), indicating that F_1 produced an intermediate amount of fruit compared with its parents, with a fruit size close to P_1. Therefore, it is not surprising that the mean total fruit dry weight per plant of F_1 was the highest at the final harvest ($P_1<P_2<F_1$), as shown in Table 3. The results indicated that F_1 has better performance than the parents, a phenomenon called heterosis.

3.2. Model-assisted analysis

Differences in the source–sink parameters for parents P_1 and P_2 and hybrid F_1 The trend of leaf thicknesses for parents P_1 and P_2 and hybrid F_1 was $P_2>P_1>F_1$ (data not shown), which was used for parameter estimation. The target data for two plants from four different sampling dates were fitted simultaneously, including the dry weights of individual organs (internode, blade, petiole and fruit) and total dry weight of each component. In total, 1 572, 1 276, and 1 236 target data points were fitted simultaneously for P_1, P_2 and F_1, respectively. The organ-level fitting results of the last two stages (S5 and S6) for P_1, P_2 and F_1 are shown in Fig. 4. Only dry weights of individual internodes, leaves, petioles and fruits of one plant were given for each sampling for clarification. The total dry weights of each organ type for stages S3–S6 are given in Fig. 5. The data of S1 and S2 were omitted because they were too tiny to display. The correlation coefficient (R^2) values between the observed and fitted values for the two parents and their hybrid F_1 were 0.97, 0.91 and 0.92, respectively (Table 4).

Fig. 3 Environmental conditions in the greenhouse: temperature, light level and daily potential evapotranspiration (PET).
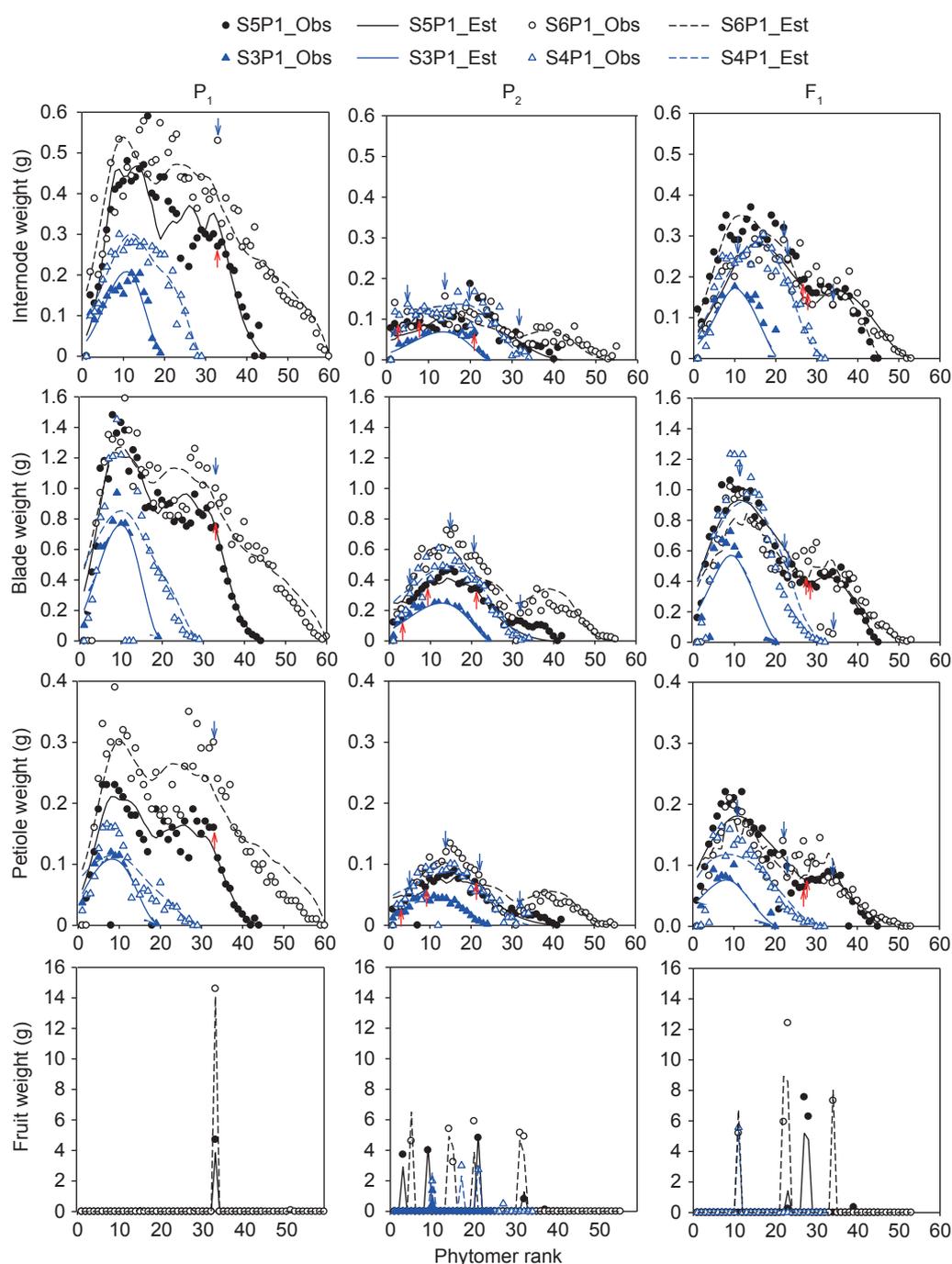
Fig. 4 Fitting results of growing stages S3 (17 May), S4 (31 May), S5 (16 June) and S6 (3 July) for two parents (P_1 and P_2) and their hybrid F_1. All the data were fitted simultaneously, including the total dry weight for all organs and organ-level dry weight of individual internodes, blades, petioles, and fruit (from top to bottom). Only one plant was given for each stage. Obs, observed data; Est, estimated data. The arrows indicate the fruit-set positions for stages S5 (up arrow) and S6 (down arrow).

Table 2 Comparison of the organ biomass and plant size for parents P_1 and P_2 and hybrid F_1 at the last stage (S6, two plants)

|	Total dry weight (g)			Average plant height (cm)	Internode diameter (mm)
	Internode	Blade	Petiole		
P_1	18.4±1.1	42.5±3.0	9.6±0.8	431.5±16	6.28±0.2
P_2	4.1±0.1	17.4±0.5	2.9±0.3	254.5±14	4.28±0.1
F_1	9.6±1.8	26.5±5.8	5.4±1.4	378.6±36	5.46±0.3

The values are expressed as mean±SD.

Table 3 Comparison of the mean final number of fruits per plant, mean dry weights of individual fruits and mean total fruit weight per plant for parents P_1 and P_2 and hybrid F_1 (growing stage S6 (3 July), two plants)

	Mean final number of fruits per plant	Mean dry weights of individual fruits (g)	Mean total fruit dry weight per plant (g)
P_1	1.0±0.7	9.6±4.9	12.2±3.5
P_2	6.0±0.9	3.9±1.8	22.9±9.1
F_1	4.2±0.8	7.2±3.4	31.9±0.6

The values are expressed as mean±SD.
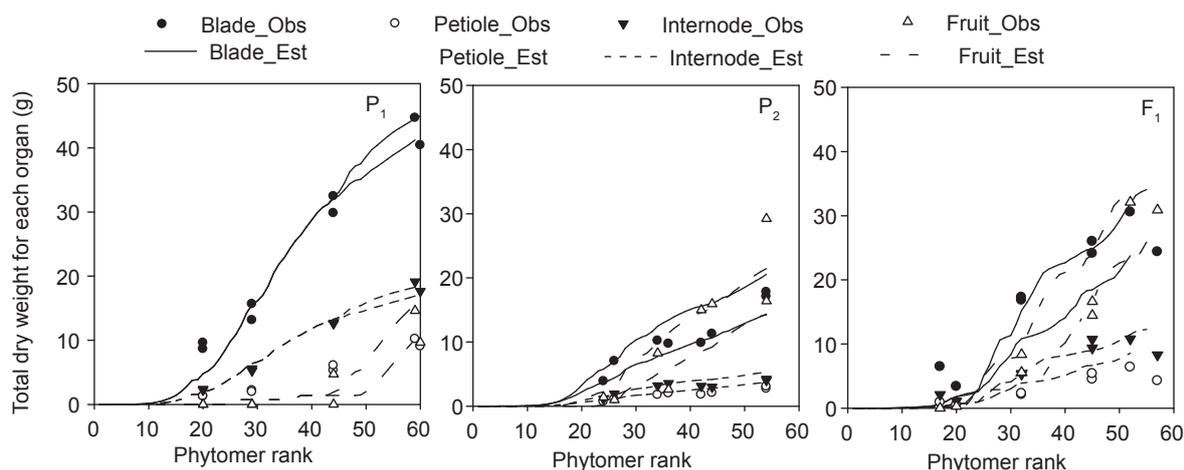
Fig. 5 Fitting results of the total dry weight for all organs by multifitting using plant data from four samplings (growing stages S3 (17 May), S4 (31 May), S5 (16 June) and S6 (3 July), respectively) for the parents (P_1 and P_2) and their hybrid F_1. Obs, observed data; Est, estimated data.

A set of source–sink parameters was identified for P_1, P_2 and F_1, as shown in Table 4. The sink strengths of the blade, petiole and internode (P_b, P_p and P_{in}) for F_1 were intermediate between those of the parents P_1 and P_2 ($P_1 > F_1 > P_2$). The sink variation of the blade (b_b) for F_1 was intermediate between that of the parents. The sink variation of the petiole (b_p) was slightly smaller than that of the parents. The sink variation values of the internode (b_{in}) and fruit (b_f) for F_1 were larger than those of P_1 and P_2, respectively, indicating quicker expansion compared with the leaves. Regarding the source parameters, the projection area (S_P) for F_1 was intermediate between that of the parents P_1 and P_2 ($P_1 > F_1 > P_2$). The water use efficiency (μ) was larger for F_1 than for P_1 and P_2 ($P_2 < P_1 < F_1$). There are shifts in the profiles of the internode and blade that were not reproduced by the model, likely due to the abortion of early fruit for parent P_1.

Computed plant biomass production, demand and source–sink ratio Using these parameter values, the plant biomass production and plant demand of each cycle were computed (Fig. 6). The biomass production per cycle (Q, Fig. 6-A) and cumulated biomass production (Fig. 6-B) were larger for parent P_1 and hybrid F_1 than for parent P_2. The plant demand (D, Fig. 6-C) was larger for parent P_2 and hybrid F_1 than for parent P_1, which was consistent with the fruit setting. Anytime there is fruit removal after maturation,

**Table 4** Estimated parameter values for parents P_1 and P_2 and hybrid F_1

Parameter[1]	P_1	P_2	F_1
P_b	0.87 (0.55)	1.66 (0.40)	1.15 (0.18)
P_p	0.18 (1.15)	0.28 (0.67)	0.21 (0.81)
P_{in}	0.36 (2.00)	0.44 (0.19)	0.41 (0.23)
b_b	2.11 (0.19)	2.76 (0.07)	2.36 (0.18)
b_p	1.81 (1.54)	2.46 (0.58)	1.66 (1.29)
b_{in}	2.67 (3.98)	2.59 (1.90)	3.46 (3.03)
b_f	1.35 (0.08)	2.41 (0.05)	5.35 (0.04)
S_P	479.0 (4.08)	134.5 (2.22)	251.9 (2.91)
μ	0.00052 (0.45)	0.00042 (0.85)	0.00069 (0.99)
R^2	0.97	0.91	0.92

[1] P_o is the coefficient of sink strength; b_o is the parameter of the beta function for organ expansion, where, o=in (internode); b (blade); p (petiole); f (fruit). S_P is the projected surface area of the plant. The sink strength of fruit (P_f) is set to their respective maximum fruit weight.
Data in parentheses are CVs (%).

the plant demand drops.

The ratio between the biomass supply and demand (Q/D, Fig. 6-D) increased during the vegetative stage until fruit began to be the dominant sinks. The peak value was first reached for parent P_2 followed by hybrid F_1 and then parent P_1. The value of the first peak of hybrid F_1 was between the two parents (P_1 and P_2). The Q/D of the parent P_1 and F_1 hybrid was visibly larger than that of P_2.
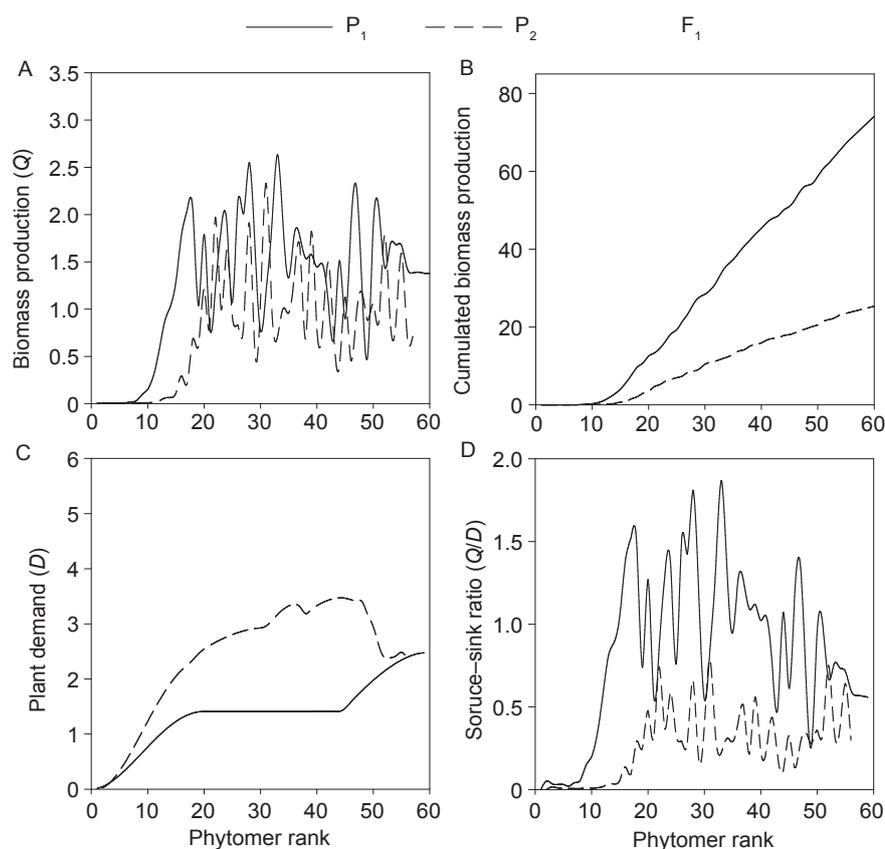
Fig. 6 Estimated values during plant growth. A, biomass production per cycle Q. B, accumulated biomass production per plant. C, plant demand per cycle D. D, plant source–sink ratio (Q/D) for the parents P_1 and P_2 and their hybrid F_1.

Large-fruited cultivar P_1 needs a higher source–sink ratio for the fruit set.

3.3. Computational experiments on the fruit weight

Optimizing fruit positions and numbers Based on the estimated source–sink parameters, the positions of fruit are optimized by setting different number of fruit per plant for the parents P_1 and P_2 and hybrid F_1 to analyze the effect of the sink organ on potential fruit weights. Here, the potential fruit weight means the best yield with different fruit positions. It increased with the number of fruits per plant and reached the saturation point at approximately 10 fruit (Fig. 7-A) for the parents P_1 and P_2 and hybrid F_1, while the average fruit weight decreased (Fig. 7-B). The optimized values of the parent P_1 and hybrid F_1 were larger than that of parent P_2, indicating a higher source supply in P_1 and F_1. The total potential biomass production of P_1 and F_1 are close, depending on the source parameters (S_P and μ). The increase in biomass production reached a limit, indicating a limit in the source supply. Interestingly, the potential and observed plant biomass are close for the parent P_2 (6 fruits) and hybrid F_1 (4 fruits), with 29.3 g *vs*. 29.7 g (increase by

1%) and 32.4 g *vs*. 35.7 g (increase by 10%), respectively. This could mean that, for a real plant, its fruit position is already optimized by itself for its biomass production. This result agrees with that in a previous study of the fruit position optimization of maize (Qi *et al*. 2009).

Optimizing the fruit positions, numbers and source–sink parameters Both the source–sink parameters and positions of the fruit per plant were synchronously optimized using different numbers of fruits per plant to check the potential augmentation of biomass. Here, the potential plant was obtained by synchronously optimizing the source–sink parameters and numbers and positions of the fruits per plant. Table 5 gives the variation in the optimized parameters, which is limited to the range between the estimated values (Table 4) of the parents and F_1 hybrid.

As shown in Fig. 8, both the optimized total and average fruit weights were larger than the observed values. This is reasonable because the source capacity increased. The optimized total fruit weights increased with the fruit number and reached a saturation point of approximately 10 fruits. The mean fruit weights decreased but were always above the observed values. The optimized source parameter (S_P) was close to the value of parent P_1, while the source parameter
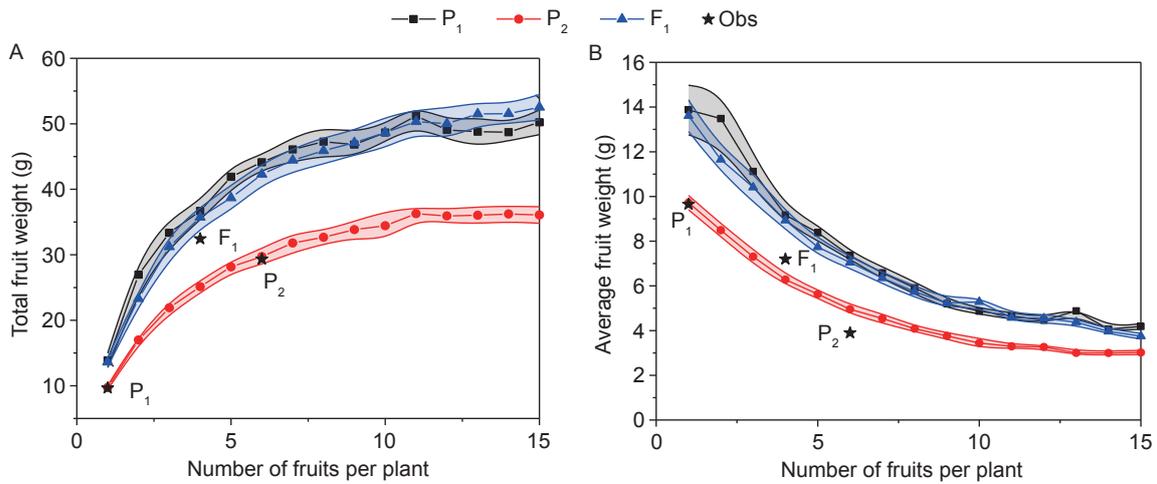
Fig. 7 Optimized and observed (Obs) total weight (A) and average weight (B) of fruit for the fruit number range from 1 to 15 when the fruit position is optimized. The area around each fruit weight corresponds to the respective standard error.

Table 5 Definitions and variation ranges of the source–sink parameters that are optimized in the optimization problem

Parameter	Definition	Range
P_b	Sink strength of the blade	[0.5, 1.7]
P_p	Sink strength of the petiole	[0.1, 0.3]
P_{in}	Sink strength of the internode	[0.3, 0.5]
S_p	Projected surface area of the plant	[100, 500]
r	Water use efficiency	[0.0004, 0.001]
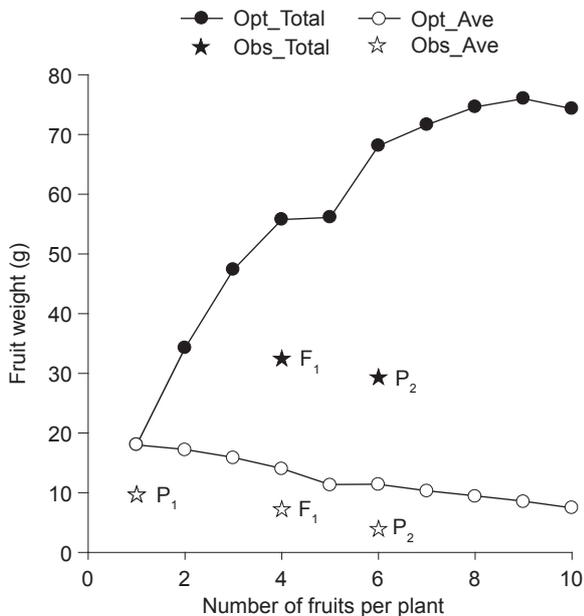
Fig. 8 Optimized (Opt) and observed (Obs) total weight and average (Ave) weight of fruits for the fruit number ranging from 1 to 10 when the fruit position and the source–sink parameters (S_p, μ, P_b, P_{in}, and P_p) are optimized. The stars represent the observed fruit weights for the parents P_1 and P_2 and F_1 hybrid.

(μ) was similar to that of hybrid F_1 (data not shown). The optimized results led to more biomass production according to eq. (1) and, thus, a larger fruit weight.

4. Discussion

The GreenLab Model was used to study the source–sink dynamics of individual organ growth and link it to the fruit setting and fruit biomass for the parents and hybrid F_1. Our modeling results confirmed that the organ growth and fruit setting is controlled by the source–sink ratio in cucumber (Fig. 6), and the model can well reproduce the results of experimental measurements. One original aspect of this study compared with earlier GreenLab models (Mathieu et al. 2007; Kang et al. 2011) was to introduce the potential fruit growth rate (measured maximum fruit dry weight) into the GreenLab model to represent the fruit sink strength. The sink strength of each organ then has units (g per GC) and represents the ability to compete for assimilates instead of a relative value (compared with the leave).

4.1. Correlation between the cyclic patterns of organ growth and source–sink ratio by the GreenLab Model

The biomass and size of each organ differ within one plant for two parents and F_1 hybrid, which could be due to the difference in the supply and demand, that is, the source–sink ratio during plant growth. Additionally, the biomass and size of each organ are different at the same phytomer rank for two parents and F_1 hybrid, likely due to the difference in their sink strengths because the expansion time showed no significant difference according to the observations.

Moreover, the waves in the organ profile appeared as an emergent property because of the fruit setting (Fig. 4), a finding that is consistent with the study of Mathieu et al. (2007). There is a time lag between an increase in the source–sink ratio (and, hence, larger leaves) and the number of young fruit because it takes time for the fruit to expand.

Furthermore, the individual fruit weight and final fruit number differ between two parents and F_1 hybrid, likely due to the difference in the fruit sink strength and source–sink ratio during the fruit setting (Marcelis et al. 2004). A general pattern is that a decrease in the source–sink ratio is accompanied by a new non-aborted fruit, and vice versa. What is interesting is the threshold (s_{low}) of setting the first and the subsequent fruit in P_1, P_2 and F_1. Fig. 6-D shows that the source–sink ratio was higher for single-fruit type P_1 and lower for multiple-fruit type P_2, while their hybrid was intermediate. This finding demonstrates that different cultivars may have different needs of the source–sink threshold (or hormone level) for the fruit setting, which gives different final numbers and sizes of fruit (Mathieu et al. 2008). This result is consistent with that of previous studies, and the link between the fruit set and computed source–sink ratio has been presented by previous application of GreenLab to sweet pepper for six cultivars (Ma et al. 2011) and tomato for different densities (Kang et al. 2011).

4.2. Model-assisted analysis of biomass production in cucumber

According to the estimated parameters of source strength (S_P and μ) and sink strength (P_{in}, P_b and P_p), we can see that the model explained well the differences in biomass production for P_1, P_2 and F_1. The estimated sink parameters of the internode (P_{in}), blade (P_b) and petiole (P_p) in F_1 plants were intermediate between the parents (Table 4). The estimated results are consistent with the experimental data. Hybrid F_1 has the best fruit biomass, indicating heterosis of F_1. The high biomass production of the F_1 hybrid is achieved by factors both in plant development (fruit setting) and sink competition (larger sink strength of fruit).

The hybrid F_1 has close features of assimilate productivity with P_1, with large leaves and, hence, huge source strength. On the other hand, the assimilate utility of F_1 is increased by producing more fruit than P_1 and larger fruit than P_2 (7.2 g more on average). Therefore, a high biomass production of F_1 plants is a result of delicate optimization of the source and sink strength, and high biomass production requires both high assimilate productivity and high assimilate utility.

4.3. Computational experiments on fruit weight

According to eq. (1), the larger the source parameters (S_P and μ), the more the assimilate supply (biomass production). These two parameters are related to environmental factors, such as temperature and light (Fig. 3). The sink parameters of internode (P_{in}), blade (P_b) and petiole (P_p) and the maximum fruit weight mainly depend on genetic factors.

The optimization results also revealed the relationship between the source–sink ratios and fruit-setting for cucumber (Figs. 7 and 8). The increase in fruit weight results from the increased sink strength and proportion of plant biomass allocation for fruits. On one hand, plant demand is the sum of all the organ sinks, as described in eq. (4), and the increase in sink strength can lead to an increase in fruit weight. On the other hand, the increase in biomass allocation depends on the leaf surface area (S_P) and water use efficiency (r).

When we set the fruit number to their corresponding observed value for two parents and F_1 hybrid, the optimized fruit weight results are consistent with the observed values. Moreover, the hybrid F_1, which is a hybrid between the parents P_1 and P_2, may already be close to the optimum regarding fruit biomass. Thus, the equilibrium of the source and sink for the functional parts is adjusted by its structure (fruit numbers and positions), and the plant can adjust itself by self-optimization.

Furthermore, the potential fruit weights increased with the number of fruit per plant and reached the saturation point at approximately 10 fruit (Fig. 7-A), indicating that a limit of source supply exists. Therefore, to increase the yield, not only the number of fruits per plant but also the source supply needs to be considered. Additionally, to obtain the maximal fruit weight, the optimal trade-offs between the sources and sinks should be considered. The optimization results indicated that the growers should tend to have more fruit on their plants. However, the economic value of cucumber fruit also depends on their average size. Thus, a minimal threshold should be given in the model below, indicating that the fruit cannot be sold to customers.

4.4. Application of the GreenLab Model to genetic selection

Genotype×environment interactions are unavoidable in plant multienvironment trials. The use of a plant growth and development modeling framework can link phenotype complexity to underlying genetic systems in a way that enhances the power of molecular breeding strategies (Yin et al. 2016). The potential of linking the GreenLab Model to quantitative genetics has been studied (Letort et al. 2008). Moreover, it is possible to simulate the complex plasticity of plant architectural and functional responses to environmental factors using GreenLab (Vavitsara et al. 2017). Indeed, in GreenLab, the Q/D ratio can be considered an index of plant

vigor and can in particular reflect the environmental impact on plant growth, in combination with its genome effect (Letort *et al*. 2008). However, this study is just a preliminary work, and more simulations and analyses of the experimental data are needed to provide a further study of QTL detection on model parameters *vs*. phenotypic traits.

5. Conclusion

By identifying the parameters of two parent cultivars (P_1 and P_2) and their hybrid (F_1), the internal source–sink ratio was computed, and its relationship with the fruit-setting was investigated. The results indicated that the F_1 hybrid obtained heterosis by inheriting the advantages of vegetative growth and assimilate accumulation from parent P_1 and the fruit setting from parent P_2. The parameter values of F_1 show mostly additivity (the parameters of sink strength). Higher biomass production occurs owing to an optimal combination of the source and sink functions. The optimization problem investigates the optimal source–sink dynamics, and the results provide a reference for model validation, which can be seen as an assisting verification for our model. Future work involves combining this model with a genetic model to more deeply understand the genetic factors and provide guidance for plant breeders.

Acknowledgements

Appendix associated with this paper can be available on http://www.ChinaAgriSci.com/V2/En/appendix.htm

References

Allen R G, Pereira L S, Raes D, Smith M. 1998. *Crop Evapotranspiration — Guidelines for Computing Crop Water Requirements*. *FAO Irrigation and Drainage Paper No. 56*. Food and Agriculture Organization, Rome.

Birchler J A. 2015. Heterosis: The genetic basis of hybrid vigour. *Nature Plants*, **1**, 15020.

Chew Y H, Seaton D D, Millar A J. 2017. Multi-scale modelling to synergise plant systems biology and crop science. *Field Crops Research*, **202**, 77–83.

Christophe A, Letort V, Hummel I, Cournède P H, de Reffye P,

Lecoeur J. 2008. A model-based analysis of the dynamics of carbon balance at the whole-plant level in *Arabidopsis thaliana*. *Functional Plant Biology*, **35**, 1147–1162.

Falster D S, Westoby M. 2003. Leaf size and angle vary widely across species: What consequences for light interception? *New Phytologist*, **158**, 509–525.

Fan X R, Kang M Z, Heuvelink E, de Reffye P, Hu B G. 2015. A knowledge-and-data-driven modeling approach for simulating plant growth: A case study on tomato growth. *Ecological Modelling*, **312**, 363–373.

Ghaderi A, Lower R L. 1978. Heterosis and phenotypic stablility of F₁ hybrids in cucumber under controlled environment. *Journal of the American Society for Horticultural Science*, **103**, 275–278.

Guo Y, Ma Y T, Zhan Z G, Li B G. 2006. Parameter optimization and field validation of the functional-structural model GREENLAB for maize. *Annals of Botany*, **97**, 217–230.

Hammer G L, Chapman S, van Oosterom E, Podlich D W. 2005. Trait physiology and crop modelling as a framework to link phenotypic complexity to underlying genetic systems. *Australian Journal of Agricultural Research*, **56**, 947–960.

Hayes H K, Jones D F. 1916. First generation crosses in cucumbers. In: *Report of the Connecticut Agricultural Experiment Station*. Connecticut Agricultural Experiment Station, United States. pp. 319–322.

Heuvelink E, Marcelis L F M, Bakker M J, van der Ploeg A. 2007. Use of crop growth models to evaluate physiological traits in genotypes of horticultural crops. In: Spiertz J H J, Struik P C, Van Laar H H, eds., *Scale and Complexity in Plant Systems Research*: *Gene-Plant-Crop Relations*. Dordrecht, Dordrecht. pp. 223–233.

Kang M Z, Heuvelink E, Carvalho S M P, de Reffye P. 2012. A virtual plant that responds to the environment like a real one: The case for chrysanthemum. *New Phytologist*, **195**, 384–395.

Kang M Z, Yang L L, Zhang B G, de Reffye P. 2011. Correlation between dynamic tomato fruit-set and source–sink ratio: A common relationship for different plant densities and seasons? *Annals of Botany*, **107**, 805–815.

Letort V, Mahe P, Cournede P H, de Reffye P, Courtois B. 2008. Quantitative genetics and functional–structural plant growth models: Simulation of quantitative trait loci detection for model parameters and application to potential yield optimization. *Annals of Botany*, **101**, 1243–1254.

Ma Y T, Wen M P, Guo Y, Li B G, Cournède P H, de Reffye P. 2008. Parameter optimization and field validation of the functional–structural model GREENLAB for maize at different population densities. *Annals of Botany*, **101**, 1185–1194.

Ma Y T, Wubs A M, Mathieu A, Heuvelink E, Zhu J Y, Hu B G, Cournède P H, de Reffye P. 2011. Simulation of fruit-set and trophic competition and optimization of yield advantages in six *Capsicum* cultivars using functional–structural plant modelling. *Annals of Botany*, **107**, 793–803.

Marcelis L F M. 1992. The dynamics of growth and dry matter distribution in cucumber. *Annals of Botany*, **69**, 487–492.

Marcelis L F M. 1994. A simulation model for dry matter partitioning in cucumber. *Annals of Botany*, **74**, 43–52.

Marcelis L F M, Heuvelink E, Baan Hofman-Eijer L R, Den Bakker J, Xue L B. 2004. Flower and fruit abortion in sweet pepper in relation to source and sink strength. *Journal of Experimental Botany*, **55**, 2261–2268.

Mathieu A, Cournède P H, Barthélémy D, de Reffye P. 2008. Rhythms and alternating patterns in plants as emergent properties of a model of interaction between development and functioning. *Annals of Botany*, **101**, 1233–1242.

Mathieu A, Zhang B, Heuvelink E, Liu S J, Cournède P H, de Reffye P. 2007. Calibration of fruit cyclic patterns in cucumber plants as a function of source–sink ratio with the GreenLab model. In: *The 5th International Workshop on Functional–Structural Plant Models.* Napier, New Zealand. pp. 31–34.

Qi R, Ma Y T, Hu B G, de Reffye P, Cournède, P H. 2010. Optimization of source–sink dynamics in plant growth for ideotype breeding: A case study on maize. *Computer and Electronics in Agriculture*, **71**, 96–105.

Sarlikioti V, de Visser P H B, Buck-Sorlin G H, Marcelis L F M. 2011. How plant architecture affects light absorption and photosynthesis in tomato: Towards an ideotype for plant architecture using a functional–structural plant model. *Annals of Botany*, **108**, 1065–1073.

Seidel S J, Palosuo T, Thorburn P, Wallach D. 2018. Towards improved calibration of crop models — Where are we now and where should we go? *European Journal of Agronomy*, **94**, 25–35.

Vavitsara M E, Sabatier S, Kang M Z, Ranarijaona H L T, Reffye P D. 2017. Yield analysis as a function of stochastic plant architecture: Case of Spilanthes acmella in the wet and dry season. *Computers & Electronics in Agriculture*, **138**, 105–116.

Vile D, Garnier E, Shipley B, Laurent G, Navas M L, Roumet C, Lavorel S, DÍAz S, Hodgson J G, Lloret F, Midgley G F, Poorter H, Rutherford M C, Wilson P J, Wright L J. 2005. Specific leaf area and dry matter content estimate thickness in laminar leaves. *Annals of Botany*, **96**, 1129–1136.

Vos J, Evers J B, Buck-Sorlin G H, Andrieu B, Chelle M, de Visser P H B. 2010. Functional–structural plant modelling: a new versatile tool in crop science. *Journal of Experimental Botany*, **61**, 2101–2115.

Vos J, Marcelis L F M, Evers J B. 2007. Functional–structural plant modelling in crop production: Adding a dimension. In: Vos J, Marcelis L F M, de Visser P H B, Struik P C, Evers J B, eds., *Functional–Structural Plant Modelling in Crop Production*. Springer, Dordrecht. pp. 1–12.

Wright I J, Westoby M. 2002. Leaves at low versus high rainfall: Coordination of structure, lifespan and physiology. *New Phytologist*, **155**, 403–416.

Wu L, Le Dimet F X, de Reffye P, Hu B G, Cournede P H, Kang M Z. 2012. An optimal control methodology for plant growth-case study of a water supply problem of sunflower. *Mathematics and Computers in Simulation*, **82**, 909–923.

Wubs A M, Ma Y, Heuvelink E, Marcelis L F M. 2009. Genetic differences in fruit-set patterns are determined by differences in fruit sink strength and a source: Sink threshold for fruit set. *Annals of Botany*, **104**, 957–964.

Xie F L, Zhang X C, Li F, Chen W Z. 2009. Research on Heredity trend of morphological charactersof tomato germplasm resources. *Chinese Agricultural Science Bulletin*, **25**, 259–266.

Xu L F, Henke M, Zhu J, Kurth W, Buck-Sorlin G. 2011. A functional–structural model of rice linking quantitative genetic information with morphological development and physiological processes. *Annals of Botany*, **107**, 817–828.

Yan H P, Barczi J F, de Reffye P, Hu B G, Jaeger M, Roux J L. 2002. Fast algorithms of plant computation based on substructure instances. In: *International Conferences in Central Europe on Computer Graphics*. Schloss Dagstuhl, Germany.

Yan H P, Kang M Z, de Reffye P, Dingkuhn M. 2004. A dynamic, architectural plant model simulating resource-dependent growth. *Annals of Botany*, **93**, 591–602.

Yin X, Struik P C, Gu J, Wang H. 2016. Modelling QTL-trait-crop relationships: Past experiences and future prospects. In: Yin X, Struik P C, eds., *Crop Systems Biology*: *Narrowing the Gaps Between Crop Modeling and Genetics*. Springer International Publishing, Cham. pp. 193–218.

Zhan Z G, de Reffye P, Houllier F, Hu B G. 2003. Fitting a functional–structural growth model with plant architectural data. In: *Proceedings PMA03: The First International Symposium on Plant Growth Modeling, Simulation, Visualization and their Applications*. Tsinghua University Press, Springer, Beijing, China.